Applied Catalysis B: Environmental 90 (2009) 587–594

Contents lists available at ScienceDirect

Applied Catalysis B: Environmental

journal homepage: www.elsevier.com/locate/apcatb

Biodiesel production from soybean oil catalyzed by multifunctionalized Ta_2O_5/SiO_2-[$H_3PW_{12}O_{40}$/R] (R = Me or Ph) hybrid catalyst

Leilei Xu, Wei Li, Jianglei Hu, Xia Yang, Yihang Guo *

School of Chemistry, Northeast Normal University, Changchun 130024, PR China

ARTICLE INFO

Article history:
Received 8 November 2008
Received in revised form 19 January 2009
Accepted 16 April 2009
Available online 23 April 2009

Keywords:
Organic–inorganic hybrid catalyst
12-tungstophosphoic acid
Tantalum oxide
Transesterification
Esterification
Biodiesel

ABSTRACT

Mesoporous Ta_2O_5 materials functionalized with both alkyl group and a Keggin-type heteropoly acid, Ta_2O_5/SiO_2-[$H_3PW_{12}O_{40}$/R] (R = Me or Ph), was prepared by a single step sol–gel co-condensation method followed by a hydrothermal treatment in the presence of a triblock copolymer surfactant. The catalytic performance of the resulting multifunctionalized organic–inorganic hybrid materials was evaluated by a direct use of soybean oil for biodiesel production in the presence of 20 wt% myristic acid under atmosphere refluxing, and the influences of the catalyst preparation approaches, functional component loadings, and molar ratios of oil to methanol on the catalytic activity of the Ta_2O_5/SiO_2-[$H_3PW_{12}O_{40}$/R] were studied. In addition, the recyclability of the hybrid materials was evaluated via four catalytic runs. Finally, the network structures of the hybrid materials and the functions of the incorporated alkyl groups on the catalytic activity of the materials were put forward.

© 2009 Elsevier B.V. All rights reserved.

1. Introduction

Transesterification of vegetable oils with short chain alcohols to form fatty acid methyl esters (FAMEs, main components of biodiesel) has been a focus of much recent research because of the need to replace fossil fuel energy sources with renewable biofuels [1–5]. However, the commercialization of biodiesel production has seldom been realized so far due to the high cost of the feedstocks (e.g. virgin vegetable oil), which accounts for 88% of the total estimated production [6]. The problem is expected to be overcome by using low cost feedstocks like waste cooking oils, but the application of these feedstocks is a challenge because of the presence of undesirable components such as free fatty acids (FFAs) and water [6,7–9]. These components make the conventional base-catalyzed transesterification route inappropriate owing to soap formation, which results in a severe problem of the product separation and ultimately lowers the FAME yields substantially. For feedstocks with high FFA content, acid catalysis is preferable to base catalysis because it allows the simultaneous esterification of FFAs and transesterification of triglycerides under the appropriate reaction conditions without the formation of soap, as a consequence, the biodiesel manufacturing process would be further simplified [1,3,6]. However, the inherent drawbacks for the use of liquid acid catalysts such as slow reaction rate, requirement of high temperature, high molar ratio of oil and alcohol, separation of the catalyst, and serious environmental and corrosion related problems make their applications non-practical for biodiesel production [1].

Solid acid catalysts, which are recyclable and readily separable from the reaction system, offer the opportunity to reduce the impact on environment and increase industrial interest for biodiesel production [10,11]. As one of super strong Brønsted acids, heteropoly acid (HPA), in particular the Keggin-type 12-tungstophosphoric acid, possesses potential economic and green benefits for biodiesel production. And the disadvantages of HPA including small specific surface area and high solubility in polar media can be overcome by dispersing it within the inorganic porous materials [12–14]. To date, the application of the Keggin unit for biodiesel synthesis usually has been performed under higher temperature or higher pressure, which made the process uneconomic thereby limiting the practical application of HPA for biodiesel production. As an example, Dalai and co-workers has reported that the hydrous zirconia supported $H_3PW_{12}O_{40}$ is a promising catalyst for the production of biodiesel from low quality oils with high FFA content; however, in order to obtain considerably high ester yields, high temperature and high pressure (200 °C, 600 psi) were applied throughout the biodiesel production process [15]. Therefore, the development of the biodiesel production process catalyzed by novel water-tolerant HPAs under mild conditions is still a challenge. Our previous work has reported a Ta_2O_5 supported $H_3PW_{12}O_{40}$ composite catalyst ($H_3PW_{12}O_{40}$/Ta_2O_5) with a 3D interconnected mesoporous structure, and it exhibits considerably high catalytic activity, selectivity, and stability towards the simultaneous esterification of lauric acid/

* Corresponding author. Tel.: +86 431 85098705; fax: +86 431 85098705.
E-mail address: guoyh@nenu.edu.cn (Y. Guo).

0926-3373/$ – see front matter © 2009 Elsevier B.V. All rights reserved.
doi:10.1016/j.apcatb.2009.04.020

myristic acid and transesterification of tripalmitin with methanol under mild conditions. Selecting Ta_2O_5 as the support is due to its acidic property, and its acid strength can be further improved by incorporating with $H_3PW_{12}O_{40}$ due to the formation of ($\equiv$Ta-OH_2)$_n^+$($H_2PW_{12}O_{40}$)$^{n-}$ species *via* Ta–O–W bonds, which facilitated the esterification as well as transesterification reaction performing under mild conditions with high ester yields [16].

However, the presence of significant quantities of water (coming from feedstocks and from the FFA esterification reaction) in the reaction system inhibits the reactants from approaching the active sites effectively and thereby slows down the esterification reaction rate. This effect is exacerbated due to the hydrophilicity of the $H_3PW_{12}O_{40}/Ta_2O_5$ catalyst. For the transesterification reaction, the strong adsorption of the hydrophilic glycerol product on the $H_3PW_{12}O_{40}/Ta_2O_5$ surface severely limits the adsorption and diffusion of hydrophobic waste oil or triglyceride within the channels of the catalysts, leading to low catalytic activity of the catalysts; meanwhile, this strong adsorption of glycerol on the $H_3PW_{12}O_{40}/Ta_2O_5$ surface results in catalyst deactivation in some extents, which has been found during the process of recycling uses of the catalyst. Therefore, the catalytic performance of $H_3PW_{12}O_{40}/Ta_2O_5$ for both esterification and transesterification reactions is expected to be improved further by increasing its hydrophobicity or tuning hydrophobic/hydrophilic balance, accordingly, easy desorption of glycerol and efficient adsorption of oil or triglyceride on the catalyst surface can be realized simultaneously. Similar work has been reported by some research groups. For example, Corma and co-workers reported that significantly high activity of USY catalysts in the esterification of benzoic and phenylacetic acids with short-chain alcohols was attributed to its inherent hydrophobicity [17]; Shank and co-workers found that the catalytic activity of esterification of palmitic acid in soybean oil with short-chain alcohols was improved by modification of sulfonic acid-functionalized mesoporous silica with hydrophobic alkyl groups [18]. These results suggest that the hydrophobic surface of the catalyst can enhance the adsorption capacity of the hydrophobic oily species and avoid possible deactivation of the active sites via weakening glycerol adsorption as well as exclude water continuously from the pore channels. Up to date, there are no reports on the utilization of this kind of multifunctionalized materials for catalyzing esterification and transesterification reactions in one step.

Herein, the enhancement of the hydrophobicity of $H_3PW_{12}O_{40}/Ta_2O_5$ is accomplished by modifying it with hydrophobic alkyl groups such as methyl or phenyl. The preparation of this 3D interconnected mesoporous organic–inorganic hybrid catalyst was performed in a single step of sol–gel co-condensation followed by a hydrothermal treatment in the presence of a triblock copolymer surfactant. For comparison, the post-synthesis method was also applied for the catalyst preparation process. The catalytic performance of as-prepared hybrid catalysts was evaluated by direct use of soybean oil for biodiesel production in the presence of 20 wt% myristic acid under atmosphere refluxing. At the same time, influences of the incorporation approaches, functional component (alkyl group or $H_3PW_{12}O_{40}$) loadings, and molar ratios of oil to methanol on the FAME yields were studied in detail. Finally, the network structures of as-prepared hybrid materials and the function of the incorporated alkyl groups on the catalytic activity were proposed.

2. Experimental

2.1. Materials

$H_3PW_{12}O_{40}{\cdot}xH_2O$, tantalum pentachloride ($TaCl_5$, 99%), P123 (M = 5800), methyltrimethoxysilane (MeTMS, 99%), and phenyltrimethoxysilane (PhTMS, 99%) were purchased from Aldrich and used without further purification. Myristic acid was obtained from Tianjin Guangfu Fine Chemical Research Institute, China. Soybean oil is food-grade. All other chemicals were analytical reagents and purchased from Beihua Fine Chemical Co., Beijing, China.

2.2. Catalyst preparation

2.2.1. Sol–gel co-condensation synthesis procedure

$TaCl_5$ (1.7 mmol) was dissolved in P123 (0.043 mmol)/ethanol (171.7 mmol) solution. After vigorous stirring the mixture for 1 h at room temperature, an aqueous $H_3PW_{12}O_{40}$ (0.0049–0.032 mmol) solution and a hydrophobic organic precursor (RTMS, R = Me or Ph) was added dropwise to the above mixture, and the resulting sol was stirred at room temperature for 1 h. The clear sol obtained was aged at 45 °C for 24 h, and then subjected to hydrothermal treatment at 80 °C for 48 h at a heating rate of 2 °C min^{-1}. The formed hydrogel was cooled at room temperature and then dehydrated slowly at 45 °C in vacuum until complete gel particulates were formed. The gel particulates were further dried in vacuum at 60 °C and 80 °C, respectively. Removal of P123 was performed by boiling ethanol extraction for 3 h, and then the product was separated by centrifugation and dried in vacuum at 45 °C for 24 h. The above procedure was repeated three times to ensure most of P123 being removed from the product. The final product is denoted as Ta_2O_5/SiO_2–[$H_3PW_{12}O_{40}(x)$/R(y)], where x and y represent $H_3PW_{12}O_{40}$ loading (%) and molar ratio of Ta to RTMS, respectively; herein, x = 0%, 7.0%, 10.0%, and 14.3%, respectively, determined by a Leeman Prodigy Spec inductively coupled plasma atomic emission spectrometer (ICP-AES), and y = 1, 3, 6, and 9, respectively. The reference catalysts, $H_3PW_{12}O_{40}(10.8)/Ta_2O_5$ and SiO_2-[$H_3PW_{12}O_{40}$(9.6)/Me(3)], were also prepared with the similar procedures.

2.2.2. Post-grafting synthesis procedure

Pure ordered mesoporous Ta_2O_5 was synthesized according to the procedure described in literature [19]. The dried Ta_2O_5 (0.68 mmol) was suspended in a mixture of RTMS (22.5 mmol L^{-1}), 1), $H_3PW_{12}O_{40}$ (5.5 mmol L^{-1}), and ethanol (20 mL) and then refluxed for 24 h. The product was dried at 45 °C for 24 h, and 120 °C for 2 h in vacuum, respectively. The products are represented by [$H_3PW_{12}O_{40}(x)$/R(3)]–Ta_2O_5/SiO_2. Loading of $H_3PW_{12}O_{40}$ in [$H_3PW_{12}O_{40}(x)$/R(3)]–Ta_2O_5/SiO_2 composite is 7.5%, determined by ICP-AES.

2.3. Catalyst characterization

FT-IR spectra were recorded on a Nicolet Magna 560 IR spectrophotometer. Raman scattering spectra were recorded on a Jobin-Yvon HR 800 instrument with an Ar^+ laser source of 488 nm wavelength in a macroscopic configuration. Low- and wide-angle XRD patterns of the composites were obtained on a D/max-2200 VPC diffractometer using CuKα radiation. TEM images were obtained on a JEOL JEM-2010 transmission electron microscope at an accelerating voltage of 200 kV. Nitrogen porosimetry was performed on a Micromeritics ASAP 2010 instrument. Surface areas were calculated using the BET equation. Pore size distributions were calculated using the BJH model based on nitrogen desorption isotherms.

2.4. Testing of the catalysts

A model of waste cooking oil with high FFA contents was simulated by using 20 wt% myristic acid in soybean oil. Simultaneous esterification and transesterification was carried out using as-prepared catalysts under atmosphere refluxing (65 °C) for 24 h

in a round bottomed glass flask (25 mL) fitted with a water cooled condenser. For each reaction, 50 mg (2 wt%) of air-exposed catalyst was dispersed into the mixture of oil (2–0.5 mmol) and methanol (40–60 mmol) with a constant reaction volume (*ca.* 3.0 mL). The samples were withdrawn periodically and then centrifuged for the determination of the concentrations of the produced FAMEs on an Agilent 6890 GC fitted with a HP-INNOWax capillary column and flame ionization detector. Ethyl laurate was applied as an internal standard. Through GC–MS analysis, methyl palmitin (C16:0), methyl oleate (C18:1), methyl linoleate (C18:2), and methyl myristate (C14:0) are the main products in the above reaction system.

The performance of the catalysts was characterized quantitatively by the yields of FAME (Y %) which was calculated as follows: $Y = (M_D/M_T) \times 100$, where M_D and M_T are the number of moles of each FAME produced and expected, respectively.

2.5. Catalysts reusability and leaching tests

The catalyst separated from the reaction mixture by centrifugation was washed with dichloromethane for three times and dried at 60 °C overnight for subsequent catalytic cycles. The leaching of the catalyst into the reaction mixture was investigated by ICP-AES.

3. Results and discussion

3.1. Catalyst characterization

3.1.1. Compositional and structural information

The determined $H_3PW_{12}O_{40}$ loadings in the co-condensed hybrid catalysts are as expected, implying that the direct synthesis method employed can effectively inhibit the loss of the Keggin unit. As for the grafted hybrid catalysts, the determined $H_3PW_{12}O_{40}$ loadings are obviously lower than that of the expected values. This is due to the post-grafting preparation method applied. By using this method, the Keggin units or alkyl groups interacted preferentially at the pore openings of Ta_2O_5 support during the initial stages of the preparation process, and further diffusion of molecules into the center of the pores can be impaired, which in turn led to a non-homogeneous distribution of the functional groups within the pores and a lower degree of occupation [20].

The incorporation of the functional components in as-prepared hybrid catalysts was confirmed by FT-IR as well as Raman

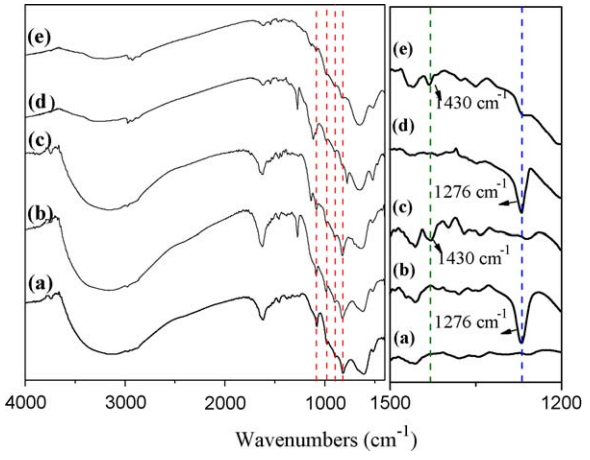

Fig. 1. FT-IR spectra of alky-free and the multifunctionalized materials prepared by one-step co-condensation and post-synthesis grafting procedure, respectively. (a) $H_3PW_{12}O_{40}(10.8)/Ta_2O_5$; (b) Ta_2O_5/SiO_2-$[H_3PW_{12}O_{40}(10.0)/Me(3)]$; (c) Ta_2O_5/SiO_2-$[H_3PW_{12}O_{40}(10.0)/Ph(3)]$; (d) $[H_3PW_{12}O_{40}(7.5)/Me(3)]$-$Ta_2O_5/SiO_2$; and (e) $[H_3PW_{12}O_{40}(7.5)/Ph(3)]$-$Ta_2O_5/SiO_2$.

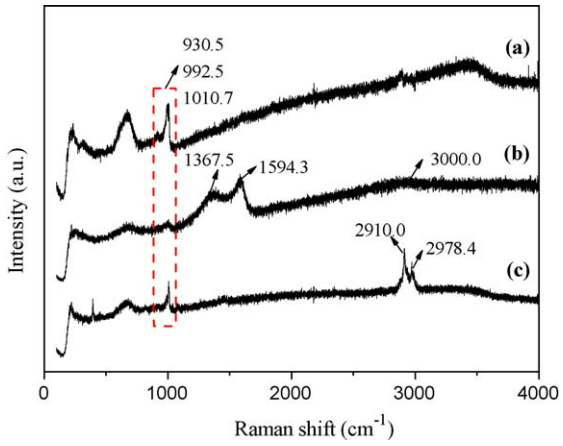

Fig. 2. Raman scattering spectra of alkyl-free and alkylated $H_3PW_{12}O_{40}/Ta_2O_5$ catalysts. (a) $H_3PW_{12}O_{40}(10.8)/Ta_2O_5$; (b) Ta_2O_5/SiO_2-$[H_3PW_{12}O_{40}(10.0)/Ph(3)]$; and (c) Ta_2O_5/SiO_2-$[H_3PW_{12}O_{40}(10.0)/Me(3)]$.

spectroscopic methods. FT-IR spectra of the hybrid materials prepared by the two methods are shown in Fig. 1. All materials exhibit characteristic vibrational frequencies related to the Keggin unit at 1080 cm^{-1}, 983 cm^{-1}, 893 cm^{-1}, and 810 cm^{-1}, respectively, attributed to stretching vibration modes of P–O, W=O, and W–O–W bonds of the Keggin unit [21]. And the presence of methyl groups bonded to silica in the hybrid materials is evidenced by the strong and sharp vibrational peak at 1276 cm^{-1} (Fig. 1b and d), characteristic of the symmetric bending mode of the methyl group in methylsilanes [22]. However, the band corresponding to the asymmetric stretching mode of this group (at *ca.* 2975 cm^{-1}) is overlapped by the strong IR absorption band of the hydroxyl group. As shown in Fig. 1c and e, the band at 1430 cm^{-1} is attributed to phenyl ring bonded to silica, confirming phenylsilanes was introduced into the hybrid materials [23].

Additional structural information concerning the presence of alkyl groups and the Keggin unit in the co-condensed hybrid catalysts was obtained from Raman scattering spectroscopy (Fig. 1). For both of the co-condensed hybrid catalysts, the peaks found at 930.5 cm^{-1}, 992.5 cm^{-1}, and 1010.7 cm^{-1} are assigned to the vibrations of W=O, W–O–W, and P–O bonds of the Keggin units (Fig. 2b and c). Additionally, the peaks identified at 3000.0 cm^{-1}, 1367.5 cm^{-1}, and 1594.3 cm^{-1} are attributed to the vibrations of aromatic C–H bonds and C–C ring, respectively (Fig. 2b) [24]; and the strong scattering peaks at 2910.0 cm^{-1} and 2978.4 cm^{-1} correspond to stretch vibrations of aliphatic C–H bonds (Fig. 2c) [24].

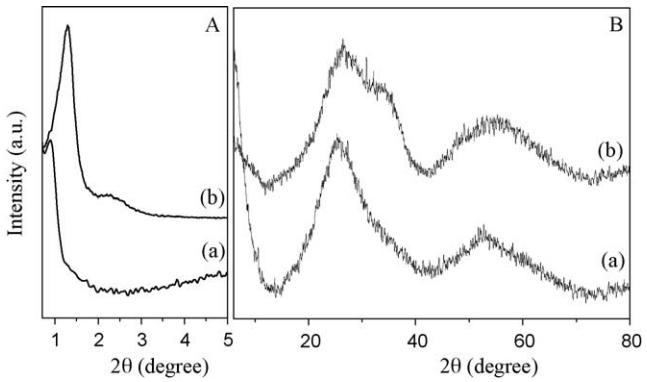

Fig. 3. Low-angle (A) and wide-angle (B) XRD patterns of the multifunctionalized materials prepared by one-step co-condensation and post-synthesis grafting procedure, respectively. (a) Ta_2O_5/SiO_2-$[H_3PW_{12}O_{40}(10.0)/Me(3)]$ and (b) $[H_3PW_{12}O_{40}(7.5)/Me(3)]$-$Ta_2O_5/SiO_2$.

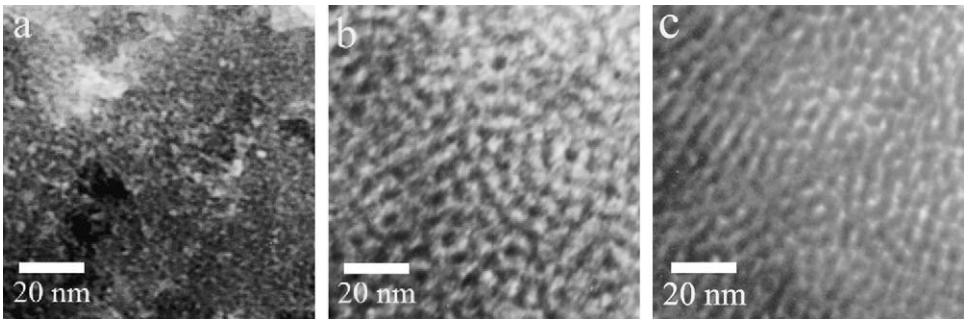

Fig. 4. TEM images of the multifunctionalized mesoporous materials synthesized by one-step co-condensation and post-synthesis grafting procedure, respectively. (a) Ta_2O_5/SiO_2-[$H_3PW_{12}O_{40}$(10.0)/Me(3)]; (b) Ta_2O_5/SiO_2-[$H_3PW_{12}O_{40}$(10.0)/Ph(3)] and (c) [$H_3PW_{12}O_{40}$(10.0)/Me(3)]-Ta_2O_5/SiO_2.

3.1.2. Mesostructure, morphology, and porosity

The mesostructure of the prepared hybrid catalysts was revealed by low-angle XRD patterns (Fig. 3A). In the range of 0.85°–1.5°, there is a main reflection peak (1 0 0) for both catalysts prepared with different methods, indicative of a mesoporous structure of the catalysts with obvious difference in *d* spacing. The grafted [$H_3PW_{12}O_{40}$(7.5)/Me(3)]–Ta_2O_5/SiO_2 sample also shows the other peak with weak intensity at *ca.* 2°–2.5° (Fig. 3A-b), suggesting long-range ordered mesostructure is expected for this sample. But the mesoporous periodicity of the co-condensed Ta_2O_5/SiO_2–[$H_3PW_{12}O_{40}$(10.0)/Me(3)] sample is considered to be poor due to lacking of the second peak in the range of 2°–2.5°. The above results indicate that the alkylated $H_3PW_{12}O_{40}/Ta_2O_5$ catalysts prepared under different routes exhibit different mesostructural properties, which is consistent with the subsequent TEM observations (Fig. 4). As shown in Fig. 3B, the wide-angle XRD patterns corresponding to the Keggin unit are not found and the two broad peaks situate at *ca.* 25° and 55° originated from amorphous Ta_2O_5. Therefore, it is confirmed that the Keggin units homogeneously dispersed throughout as-prepared hybrid materials [16].

TEM images revealed that the co-condensed samples, Ta_2O_5/SiO_2–[$H_3PW_{12}O_{40}$(10.0)/Me(3)] and Ta_2O_5/SiO_2–[$H_3PW_{12}O_{40}$(10.0)/Ph(3)], exhibited a poor ordered 3D interconnected wormhole pore structure (Fig. 4a and b); while the grafted [$H_3PW_{12}O_{40}$(7.5)/Me(3)]–Ta_2O_5/SiO_2 possessed an ordered hexagonal array of the mesopores (Fig. 4c). The different pore morphologies are closely related to the preparation routes: the post-synthesis method usually retains the ordered mesostructure of the starting support, whereas the co-condensation method decreases the periodicity of the materials thereby leading to totally disordered products [20].

The N_2 adsorption–desorption isotherms of all samples are Type IV with H2-type hysteresis loops, which is indicative of the well-distributed mesostructure of the materials tailored by non-ionic templates (Fig. 5) [13]. The BET surface area of the co-condensed hybrid catalyst, either Ta_2O_5/SiO_2-[$H_3PW_{12}O_{40}$(10.0)/Me(3)] or Ta_2O_5/SiO_2-[$H_3PW_{12}O_{40}$(10.0)/Ph(3)], is larger than that of the alkyl-free reference catalyst ($H_3PW_{12}O_{40}$(10.8)/Ta_2O_5); moreover, the phenylated Ta_2O_5/SiO_2-[$H_3PW_{12}O_{40}$(10.0)/Ph(3)] shows a little smaller BET surface area than that of the methylated Ta_2O_5/SiO_2-[$H_3PW_{12}O_{40}$(10.0)/Me(3)] (Table 1). This may be due to the steric hindrance effects of phenyl in silane, which may partially block the pore openings. The same trend is also observed for the samples synthesized by the grafted procedure, but the BET surface areas of the two samples have little change compared with that of the $H_3PW_{12}O_{40}$(10.8)-Ta_2O_5 catalyst. However, the sizes of the hysteresis loops (Fig. 5A) and pore volumes (Table 1) decrease, implying a possible accumulation of both the Keggin unit and alkyl groups around the pore openings [18]. As shown in Fig. 5B, the pore size distributions of all tested samples are unimodal, and the narrow pore size distribution curves are centred at a pore diameter of 2.9–3.5 nm. These results imply the pores within the composites are uniform, which is in good agreement with the TEM results.

3.2. Testing of the catalyst

The catalytic performance of the grafted and co-condensed hybrid catalysts were evaluated by the reactions of simultaneous esterification of myristic acid and transesterification of the soybean oil with methanol to produce FAMEs under identical reaction conditions of 65 °C, 1:90 molar ratio of oil to methanol, and 2 wt% catalysts. For comparison, the reference catalysts, SiO_2-

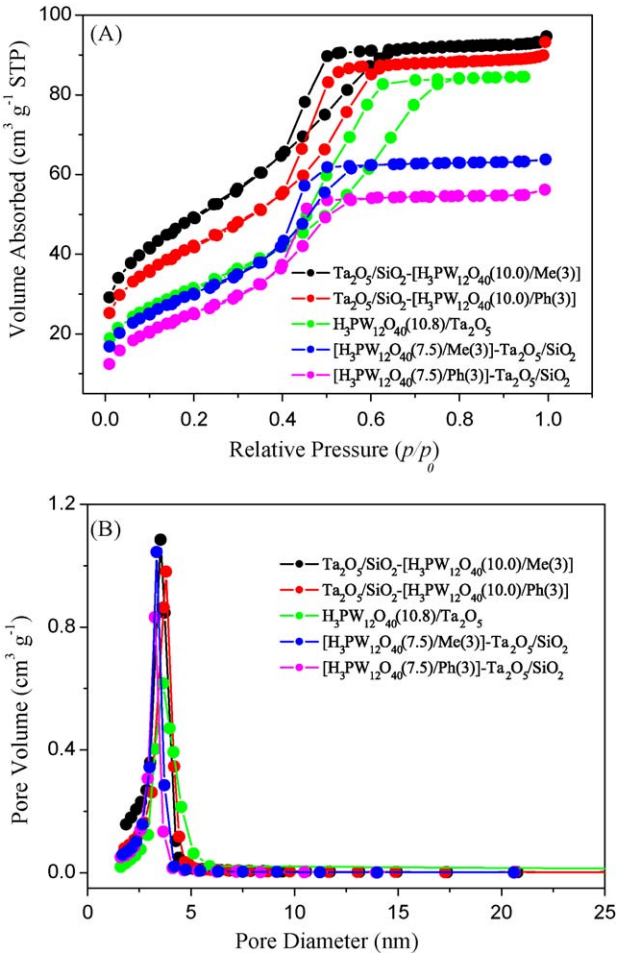

Fig. 5. Nitrogen adsorption–desorption isotherms (A) and pore size distribution profiles (B) of the multifunctionalized mesoporous materials prepared by one-step co-condendation and post-synthesis grafting procedure, respectively.

Table 1
Surface textural properties of various mesoporous hybrid catalysts and their catalytic activity towards simultaneous esterification of myristic acid and transesterification of soybean oil[a].

Catalyst	S_{BET} ($m^2\ g^{-1}$)	D_p (nm)	V_p ($cm^3\ g^{-1}$)	Ester Yield (%)			
				Methyl myristate[b]	Methyl palmitin[c]	Methyl oleate[c]	Methyl linoleate[c]
$H_3PW_{12}O_{40}$(10.8)/Ta_2O_5	114.7	5.0	0.18	54.8	24.9	20.5	30.4
Ta_2O_5/SiO_2-[$H_3PW_{12}O_{40}$(10.0)/Me(3)]	178.2	3.2	0.16	79.4	65.9	53.9	81.2
Ta_2O_5/SiO_2-[$H_3PW_{12}O_{40}$(10.0)/Ph(3)]	152.1	3.5	0.15	70.2	40.9	34.7	52.2
[$H_3PW_{12}O_{40}$(7.5)/Me(3)]-Ta_2O_5/SiO_2	110.6	3.0	0.105	13.4	2.9	2.0	3.3
[$H_3PW_{12}O_{40}$(7.5)/Ph(3)]-Ta_2O_5/SiO_2	94.3	2.9	0.090	4.6	1.2	0.9	1.5
SiO_2-[$H_3PW_{12}O_{40}$(9.6)/Me(3)]	–	–	–	27.9	10.5	16.0	9.3

[a] Reaction condition: 20 wt% myristic acid in soybean oil; 0.66 mmol soybean oil; 60 mmol methanol; 2 wt% catalyst; 65 °C.
[b] For the esterification reaction, the yield of methyl myristate was obtained after the reaction was proceeded for 30 min.
[c] For the transesterification reaction, the yields of methyl palmitin, methyl oleate, and methyl linoleate were obtained after the reaction was proceeded for 24 h.

[$H_3PW_{12}O_{40}$(9.6)/Me(3)] and $H_3PW_{12}O_{40}$(10.8)/Ta_2O_5, were also examined under the same conditions (Table 1).

The co-condensed mesoporous hybrid catalysts (Ta_2O_5/SiO_2-[$H_3PW_{12}O_{40}$(10.0)/Me(3)] or Ta_2O_5/SiO_2-[$H_3PW_{12}O_{40}$(10.0)/Ph(3)]) as well as alkyl-free co-condensed mesoporous catalyst [$H_3PW_{12}O_{40}$(10.8)/Ta_2O_5] all showed significantly high esterification reactivity, and the yield of methyl myristate reached to 79.4%, 70.2%, and 58.4%, respectively, after the reaction was proceeded for 30 min. Under the same conditions, the yield of methyl myristate was only 27.9% by using the silica-supported co-condensed hybrid mesoporous catalyst (SiO_2-[$H_3PW_{12}O_{40}$(9.6)/Me(3)]). As for the grafted mesoporous hybrid catalysts ([$H_3PW_{12}O_{40}$(7.5)/Me(3)]-Ta_2O_5/SiO_2 and [$H_3PW_{12}O_{40}$(7.5)/Ph(3)]-Ta_2O_5/SiO_2), they gave the lowest activity, with only 13.4% and 4.6% methyl myristate yields, respectively.

In the case of the transesterification reaction, the co-condensed mesoporous hybrid catalysts still exhibited the highest catalytic activity among all tested catalysts under the experimental conditions given in Table 1; moreover, the methylated Ta_2O_5/SiO_2-[$H_3PW_{12}O_{40}$(10.0)/Me(3)] was more active than that of the phenylated Ta_2O_5/SiO_2-[$H_3PW_{12}O_{40}$(10.0)/Ph(3)] with the yields of methyl palmitin, methyl oleate, and methyl linoleate of 65.9%, 53.9%, and 81.2%, respectively, after the reaction was proceeded for 24 h. This transesterification reactivity is considerably high because the reaction was performed under mild conditions (atmosphere refluxing) rather than high pressure or high temperature; moreover, the reactivity is higher compared with the reference catalysts like the alkyl-free catalyst ($H_3PW_{12}O_{40}$(10.8)/Ta_2O_5) and the grafting ones ([$H_3PW_{12}O_{40}$(7.5)/Me/(3)]-Ta_2O_5/SiO_2 or $H_3PW_{12}O_{40}$(7.5)/Ph(3)]-Ta_2O_5/SiO_2). For the two co-condensed mesoporous hybrid catalysts with different supports, SiO_2-[$H_3PW_{12}O_{40}$(9.6)/Me(3)] and Ta_2O_5/SiO_2-[$H_3PW_{12}O_{40}$(10)/Me(3)], the former was obviously less active than the latter under the same conditions. Finally, the grafted catalysts showed the lowest transesterification activity.

The above results demonstrate that the co-condensed multifunctionalized catalysts are more active with respect to the co-condensed monofunctionalized catalysts towards both esterification and transesterification reactions; and that the incorporation approaches of the functional groups as well as the types of the supports significantly affect the catalytic performance of the resulting materials. The detail explanation for the above observations is shown in Section 3.2.2.

3.2.1. Influence of the incorporation approach

The catalytic activity difference between the co-condensed and the grafted multifunctionalized hybrid materials is due to their different preparation routes. By "one-pot" method, the alkyl groups are incorporated into Ta_2O_5 network via Ta (surface)–O–Si (internal)–C bonds, resulting in Si–O bonds are then internal to the surface of the materials thereby strong interaction between the Ta_2O_5 network and RTMS are obtained (Scheme 1, right). Moreover, the route of co-hydrolyzation and -condensation of organosilanes (RTMS) with Ta source ($TaCl_5$) provides the opportunity for homogeneous dispersion of the alkyl groups and the Keggin units throughout the final products, leading to a larger contact surfaces with the reactants. At the same time, better control over the loadings of the functional groups can be obtained by the sol–gel co-condensation method [25]. Additionally, for the co-condensed multifunctionalized catalysts, $(\equiv Ta\text{-}OH_2)_n^+(H_2PW_{12}O_{40})^{n-}$ species, main acid sites of the catalysts with enhanced Brönsted acidity compared to $H_3PW_{12}O_{40}$ or Ta_2O_5 for catalyzing esterification or transesterification, were formed at the surface of the product via Ta–O–W covalent bonds [16]. The above three factors ensure the co-condensed multifunctionalized catalyst exhibiting considerably

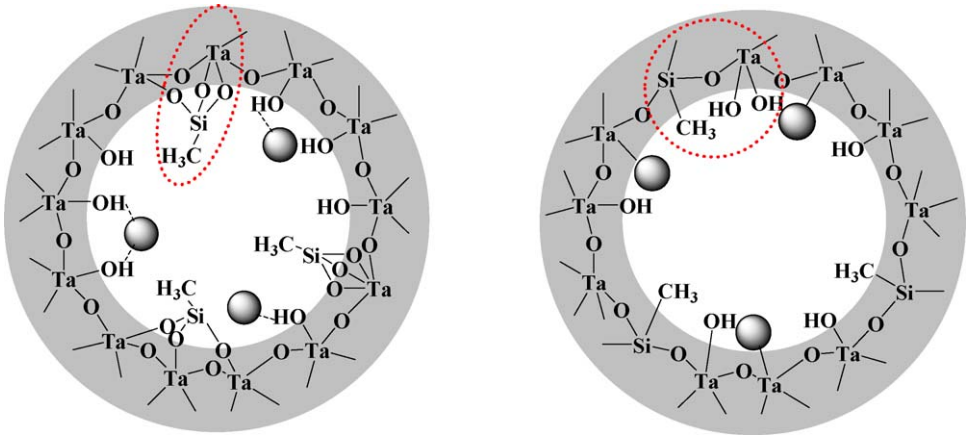

Scheme 1. Network structures of the multifunctionalized hybrid materials. (left) post-synthesis grafted [$H_3PW_{12}O_{40}$/Me]-Ta_2O_5/SiO_2; and (right) one-step co-condensed Ta_2O_5/SiO_2-[$H_3PW_{12}O_{40}$/Me]. Keggin unit.

high catalytic activity compared with the alkyl-free catalyst as well as the grafted ones (see Table 1). As for the grafted multifunctionalized catalyst, the organosilanes RTMS are covalently attached to a surface Ta atom through the Ta (surface)–O–Si (external)–C bond (Scheme 1, left). Consequently, the Si–O bonds are then external to the surface of the materials and can be cleaved during the reaction, resulting in lower activity of the catalyst [26]. Furthermore, owing to the mass transfer, Ta–OH groups on the outside and at the pore mouth of the materials would preferentially react first, resulting in pore mouth clogging. Accordingly, it is unlikely to introduce functional components into most of the mesoporous space, which significantly decreases the accessibility to the active centre as well as diffusion rate of the reactants with large molecules like triglycerides. Additionally, the weak physical interactions (e.g. hydrogen bonding) between the Keggin unit and the surface Ta–OH groups result in leaching of most of $H_3PW_{12}O_{40}$ into the reaction system (determined by ICP-AES analysis), which leads to homogeneous rather than heterogeneous catalysis with low catalytic activity. Based on the above discussion and the experimental results summarized in Table 1, we conclude that the co-condensation method is more appropriate than the grafting one for the preparation of the multifunctionalized hybrid catalysts with high catalytic activity and stability. Thus, the co-condensed multifunctionalized hybrid catalyst was used for the subsequent studies.

3.2.2. Influence of the content of alkyl groups

The influence of the content of alkyl groups on the transesterification yield of Ta_2O_5/SiO_2-[$H_3PW_{12}O_{40}$(10.0)/Me(y)] (y = 1, 3, 6, and 9) was studied at a molar ratio of oil to alcohol of 1:20 (Fig. 6). The results indicated that the Ta_2O_5/SiO_2-[$H_3PW_{12}O_{40}$(10.0)/Me(3)] catalyst showed the highest activity with the yields of methyl linoleate, methyl palmitin, and methyl oleate of 16.0%, 15.0%, and 11.5%, respectively. The catalytic activity began to decrease as the molar ratio of Ta to MeTMS was higher than 3, attributed to the increase of the hydrophilic character of the catalyst. But for the Ta_2O_5/SiO_2-[$H_3PW_{12}O_{40}$(10.0)/Me(1)] catalyst with the highest MeTMS content, its transesterification activity was also lower [27].

The enhanced catalytic activity of multifunctionalized organic–inorganic hybrid materials, Ta_2O_5/SiO_2-[$H_3PW_{12}O_{40}$/R], for the esterification and transesterification reactions with respect to the monofunctionalized $H_3PW_{12}O_{40}/Ta_2O_5$ is mainly attributed to its depletion of the hydrophilic character of the catalyst due to the presence of the alkyl groups. For the esterification reaction, it created a hydrophobic environment within pores, which served to exclude the yielded water from the active sites, leading to the catalyst to sustain higher reaction rate. As for the transesterification reaction, it tuned the hydrophobic/hydrophilic balance of the catalyst, which is beneficial to the reaction with highly hydrophobic triglycerides reactant and rather hydrophilic glycerol product. Therefore, the relative affinity of the catalyst to triglycerides and glycerol was changed, leading to relatively weak adsorption of glycerol molecules and strong adsorption of triglycerides molecules on the multifunctionalized hybrid catalyst surface. As a consequence, higher activity and much lower catalyst deactivation (see Fig. 9) were obtained compared to alkyl-free $H_3PW_{12}O_{40}/Ta_2O_5$. The above discussion is supported by the following experimental observation. When the $H_3PW_{12}O_{40}/Ta_2O_5$ was used as the transesterification catalyst, the phase separation occurred in the reaction system with transparent methanol layer and opalescent oil layer containing the catalyst; however, a uniform blend of methanol layer, oil layer, and catalyst was obtained after replacement of $H_3PW_{12}O_{40}/Ta_2O_5$ with multifunctionalized Ta_2O_5/SiO_2-[$H_3PW_{12}O_{40}$/R], leading to good contact between the acid sites and the reactants.

The function of alkyl groups in the grafted and co-condensed catalysts to the simultaneous esterification and transesterification reactions for excluding the hydrophilic product (water or glycerol) is shown in Scheme 2; for comparison, $H_3PW_{12}O_{40}/Ta_2O_5$ is also illustrated (on the top). In the case of $H_3PW_{12}O_{40}/Ta_2O_5$ catalyst, its high affinity to the hydrophilic products resulted in them strong adsorption on the catalyst surface, which would prevent oil or FFA from accessing the acidic sites and thereby inhibiting the reactions. However, incorporation of the hydrophobic alkyl groups either by co-condendation technique (in the middle) or post-synthesis grafting procedure (at the bottom) would selectively create an unsuitable environment for hydrophilic products, leading to their easy desorption from the catalyst surface, which made the proximity of the reactant molecules to the active sites easily. As shown in the middle, co-condensation route would place the hydrophobic alkyl groups within the pores and provide a more uniform dispersion of the functional groups, which prevented hydrophilic molecules from contacting with the active sites and thereby ensured sufficient contact of the reactants with the active sites. On the contrary, as for the grafted catalyst, most of the alkyl groups situated on the outside of the pores or at the pore mouth, resulting in limiting accessibility of hydrophilic molecules to the active sites inside the pores. Both of the cases provided an environment for excluding hydrophilic molecules.

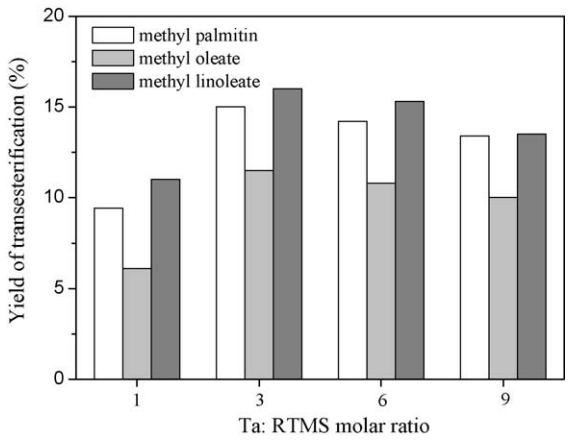

Fig. 6. Catalytic results for the transesterification of soybean oil containing 20% myristic acid with methanol catalyzed by Ta_2O_5/SiO_2-[$H_3PW_{12}O_{40}$(10.0)/Me(y)] with different Ta: RTMS molar ratios. Molar ratio of oil:MeOH = 1:20, 2 wt% catalyst, 24 h, and 65 °C.

3.2.3. Influence of $H_3PW_{12}O_{40}$ loading

To investigate the influence of $H_3PW_{12}O_{40}$ loadings on the transesterification yield, Ta_2O_5/SiO_2-[$H_3PW_{12}O_{40}$(x)/Me(3)] catalysts with x = 0%, 7.0%, 10.0%, and 14.3% were selected to catalyze transesterification of soybean oil containing 20 wt% myristic acid under a molar ratio of oil to alcohol of 1:20 (Fig. 7). By using $H_3PW_{12}O_{40}$-free Ta_2O_5/SiO_2-Me(3) catalyst, the yields of methyl linoleate, methyl palmitin, and methyl oleate were 10.9%, 9.6%, and 7.5% after the transesterification reaction proceeded for 24 h. However, the enhanced catalytic activity was obtained under same conditions by using $H_3PW_{12}O_{40}$-containing hybrid catalysts with $H_3PW_{12}O_{40}$ loadings from 7.0% to 14.3%; moreover, Ta_2O_5/SiO_2-[$H_3PW_{12}O_{40}$(10.0)/Me(3)] was the most active among the tested catalysts with the FAME yields of 16.0% (methyl linoleate), 15.0% (methyl palmitin), and 11.5% (methyl oleate), respectively. Further increasing $H_3PW_{12}O_{40}$ loading may result in a little decrease of BET surface area, as a consequence, the activity of Ta_2O_5/SiO_2-[$H_3PW_{12}O_{40}$(14.3)/Me(3)] began to decrease. Subsequent reaction was studied with Ta_2O_5/SiO_2-[$H_3PW_{12}O_{40}$(10.0)/Me(3)] for optimization of molar ratio of oil to alcohol and reusability of catalyst.

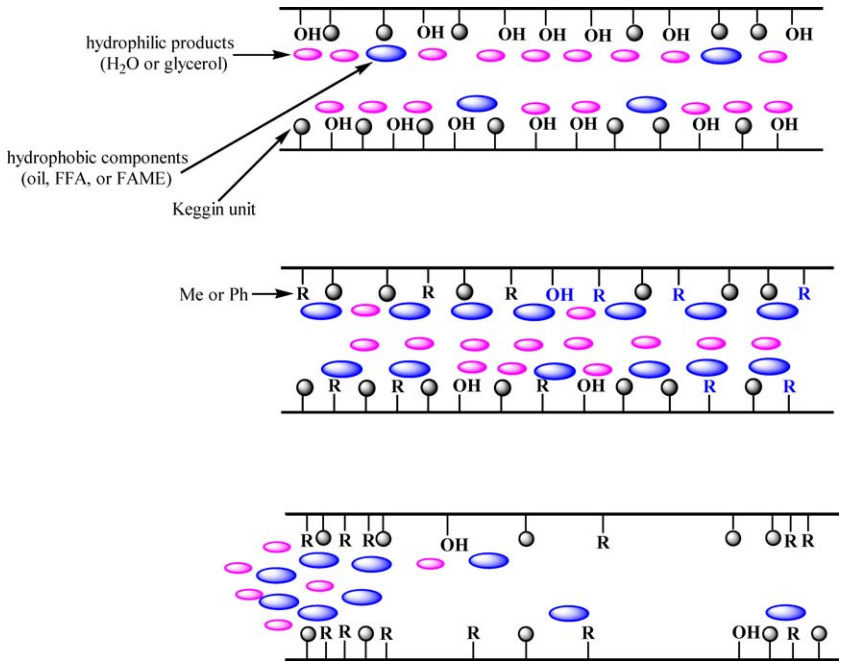

Scheme 2. Schematic representation of the influence of the surface hydrophobicity on the catalytic activity; (top) $H_3PW_{12}O_{40}/Ta_2O_5$; (middle) $[H_3PW_{12}O_{40}/R]$-Ta_2O_5/SiO_2; (bottom) $[H_3PW_{12}O_{40}/R]$-Ta_2O_5/SiO_2.

3.2.4. Influence of the molar ratio of oil to alcohol

The molar ratio of oil to alcohol is one of the most important factors to affect the ester yields. Theoretically, the esterification of 1 mol of fatty acid requires 1 mol of alcohol, while the transesterification of 1 mol of triglyceride needs 3 mol of alcohol. Since both reactions are reversible, the excess of alcohol can shift the equilibrium in the direction of ester formation [28]. It has been reported that in order to shift the equilibrium towards forward direction, the molar ratios of oil to alcohol was selected in the range of 1:40 to 1:275 [8]. Fig. 8 shows the influence of oil to methanol molar ratio on ester yields using Ta_2O_5/SiO_2-$[H_3PW_{12}O_{40}(10.0)/Me(3)]$ catalyst. An increase the oil to alcohol molar ratios from 1:20 to 1:90 resulted in a significant increase on the ester yields, but further increasing the molar ratio to 1:120 led to a decrease of the ester yields.

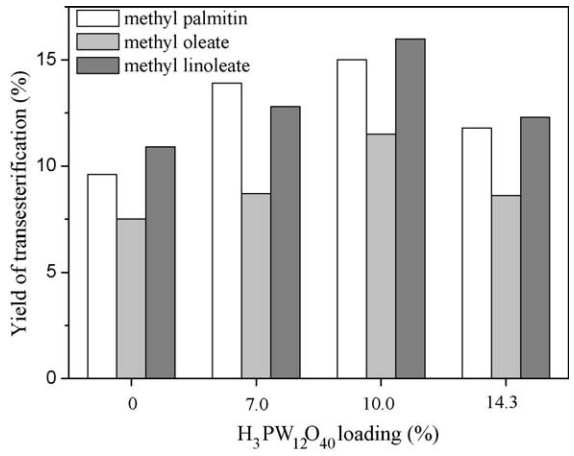

Fig. 7. Catalytic results for the transesterification of soybean oil containing 20% myristic acid with methanol catalyzed by Ta_2O_5/SiO_2-$[H_3PW_{12}O_{40}(x)/Me(3)]$ with different $H_3PW_{12}O_{40}$ loadings. Molar ratio of oil:MeOH = 1:20, 2 wt% catalyst, 24 h, and 65 °C.

3.2.5. Catalyst stability and reusability

One of the main advantages of using heterogeneous catalysts is the ease of seperation and can be reused in the successive catalytic cycles. Herein, the used Ta_2O_5/SiO_2-$[H_3PW_{12}O_{40}(10)/Me(3)]$ catalyst was separated from the reaction mixture by centrifugation and then washed with dichloromethane for three times. After being dried at 60 °C overnight, the catalyst was used for the subsequent catalytic cycles. As shown in Fig. 9, Ta_2O_5/SiO_2-$[H_3PW_{12}O_{40}(10)/Me(3)]$ showed an excellent stability and maintained a similar level of activity after four reaction cycles; meanwhile, P or W was hardly detected by ICP-AES in the catalyst-free reaction solutions. Therefore we infer that the decreases of the ester yields occurred after each catalytic cycle is possibly due to handling losses rather than leaching of active componets into the reaction media. This behaviour parallels the changes in the hydrophobicity of the catalyst, therefore, the catalyst deactivation was obviously inhibited due to easy desorption of the catalyst to glycerol.

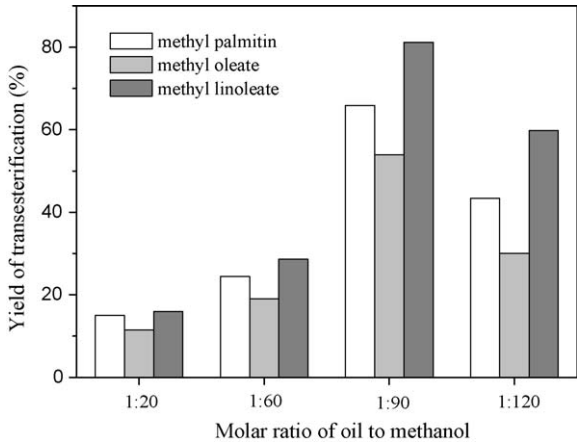

Fig. 8. Influence of oil to methanol molar ratio on transesterification reaction using Ta_2O_5/SiO_2-$[H_3PW_{12}O_{40}(10.0)/Me(3)]$ as a catalyst. 2 wt% catalyst, 24 h, and 65 °C.

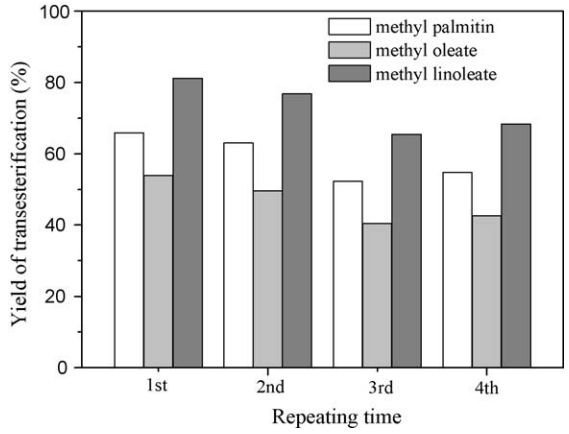

Fig. 9. Recyclability of the Ta_2O_5/SiO_2-$[H_3PW_{12}O_{40}/Me]$ for the transesterification of soybean oil with methanol in the presence of 20 wt% of myristic acid. Molar ratio of oil:MeOH = 1:90, 2 wt% catalyst, 24 h, and 65 °C.

4. Conclusion

A novel mesostructured organic–inorganic hybrid catalyst, Ta_2O_5/SiO_2-$[H_3PW_{12}O_{40}/R]$, for simultaneously catalyzing transesterification of triglycerides and esterification of FFAs in soybean oil to FAMEs was developed. Compared with alkyl-free $H_3PW_{12}O_{40}/Ta_2O_5$ catalyst, as-prepared multifunctionalized hybrid catalyst exhibited much higher catalytic activity to the above reactions; at the same time, the catalyst could be reused for four times without obvious deactivation. These unique catalytic performances of the Ta_2O_5/SiO_2-$[H_3PW_{12}O_{40}/R]$ catalyst is mainly due to the incorporation of the second functional group (methyl or phenyl) into Ta_2O_5 network except the Keggin unit. For the esterification reaction, it created a hydrophobic environment within pores thereby ensuring to exclude the yielded water from the active sites effectively; as for the transesterification reaction, it tuned the hydrophobic/hydrophilic balance of the catalyst, resulting in more efficient adsorption of triglycerides and easy desorption of glycerol. By tuning $H_3PW_{12}O_{40}$ or alkyl loading and molar ratio of oil to methanol, the highest FAME yields were obtained under mild conditions. The current studies confirm that as-prepared Ta_2O_5/SiO_2–$[H_3PW_{12}O_{40}/R]$ can function as a recyclable and robust solid acid catalyst for biodiesel production.

Acknowledgements

This work is supported by the Key Project of Chinese Ministry of Education (No. 308008), the Natural Science Fund Council of China (20873018; 50878041), the program of Changjiang Scholars and Innovative Research Team in University, and Analysis and Testing Foundation of Northeast Normal University.

References

[1] E. Lotero, Y. Liu, D.E. Lopez, K. Suwannakarn, D.A. Bruce, J.G. Goodwin Jr., Ind. Eng. Chem. Res. 44 (2005) 5353.
[2] S. Al-Zuhair, Biofuels, Bioprod. Bioref. 1 (2007) 57.
[3] K. Suwannakarn, E. Lotero, James G. Goodwin Jr., C. Lu, J. Catal. 255 (2008) 279.
[4] P. Morin, B. Hamad, G. Sapaly, M.G. Carneiro Rocha, P.G. Pries de Oliveira, W.A. Gonzalez, E. Andrade Sales, N. Essayem, Appl. Catal. A: Gen. 330 (2007) 69.
[5] A.A. Kiss, A.C. Dimian, G. Rothenberg, Adv. Synth. Catal. 348 (2006) 75.
[6] M. Di Serio, M. Cozzolino, M. Giordano, R. Tesser, P. Patrono, E. Santacesaria, Ind. Eng. Chem. Res. 46 (2007) 6379.
[7] Y. Zhang, M.A. Dubé, D.D. McLean, M. Kates, Bioresour. Technol. 89 (2003) 1.
[8] K. Jacobson, R. Gopinath, L.C. Meher, A.K. Dalai, Appl. Catal. B: Environ. 85 (2008) 86.
[9] M.G. Kulkarni, A.K. Dalai, Ind. Eng. Chem. Res. 45 (2006) 2901.
[10] T. Lacome, G. Hillion, B. Delfort, R. Revel, S. Leporc, F. Paille, FR 2855518-A1.(2005).
[11] G. Hillion, B. Delfort. I. Durand, FR 2866653-A1.(2005).
[12] N. Mizuno, M. Misono, Chem. Rev. 98 (1998) 199.
[13] Y. Guo, K. Li, X. Yu, H. James, Clark, Appl. Catal. B: Environ. 81 (2008) 182.
[14] D.P. Sawant, J. Justus, V.V. Balasubramanian, K. Ariga, P. Srinivasu, S. Velmathi, S.B. Halligudi, A. Vinu, Chem. Eur. J. 14 (2008) 3200.
[15] M.G. Kulkarni, R. Gopinath, L.C. Meher, A.K. Dalai, Green Chem. 8 (2006) 1056.
[16] L. Xu, Y. Wang, X. Yang, X. Yu, Y. Guo, J.H. Clark, Green Chem. 10 (2008) 746.
[17] A. Corma, H. García, S. Iborra, J. Primo, J. Catal. 120 (1989) 78.
[18] I.K. Mbaraka, B.H. Shanks, J. Catal. 229 (2005) 365.
[19] B. Lee, D. Lu, J.N. Kondo, K. Domen, J. Am. Chem. Soc. 124 (2002) 11256.
[20] F. Hoffmann, M. Cornelius, J. Morell, M. Fröba, Angew. Chem. Int. Ed. 45 (2006) 3216.
[21] A.D. Newman, A.F. Lee, K. Wilson, N.A. Young, Catal. Lett. 102 (2005) 45.
[22] I. Díaz, C. Márquez-Alvarez, F. Mohino, J. Pérez-Pariente, E. Sastre, J. Catal. 193 (2000) 283.
[23] Y. Li, Y. Wang, S. Ceesay, Spectrochim. Acta, Part A: Molecular and Biomolecular Spectroscopy 71 (2009) 1819.
[24] D. Lin-Vien, N.B. Colthup, W.B. Fateley, J.G. Graselli, The Handbook of Infrared and Raman Characteristic Frequencies of Organic Molecules, Academic Press, Boston, 1991.
[25] J.A. Melero, R. van Grieken, G. Morales, Chem. Rev, 106 (2006) 3790.
[26] A.P. Wight, M.E. Davis, Chem. Rev, 102 (2002) 3589.
[27] I. Díaz, C. Márquez-Alvarez, F. Mohino, J. Pérez-Pariente, E. Sastre, J. Catal. 193 (2000) 295.
[28] T.F. Dossin, M.-F. Reyniers, R.J. Berger, G.B. Marin, Appl. Catal. B: Environ. 67 (2006) 136.